

6 A microbial fuel cell sensor for unambiguous measurement of 7 organic loading and definitive identification of toxic influents

8 Martin W. A. Spurr,^a Eileen H. Yu,^b Keith Scott^b and Ian M. Head^{a*}

1 Received 00th January 20xx,
2 Accepted 00th January 20xx

3 DOI: 10.1039/x0xx00000x

9 Microbial Fuel Cells can be used as sensors to measure organic load (measured as Biochemical Oxygen Demand; BOD) in
10 aqueous wastestreams, but electrical current output can also be affected by the presence of toxic compounds. Just as BOD
11 is a non-specific measure of organic loading the toxic response is not differentiated for specific toxicants and thus enables a
12 generalised toxicity level to be monitored. To date combined BOD and toxicity sensing with a MFC has not been possible
13 without comparison with reference feeds of synthetic solutions, as a decrease in signal caused by a decrease in BOD could
14 not be distinguished from those caused by the presence of a toxicant in the waste stream. In this work, an innovative solution
15 using a three-stage MFC sensor configuration was developed to explicitly distinguish BOD-related and toxicity-related signal
16 decrease. A decrease in BOD led to an initial responses in the third, followed by the second and first stage MFC. For a
17 decrease from 360 to 60 mg/L O₂ BOD₅ the decrease in normalised current density was 59%, 82% and 94% in the first, second
18 and third MFC respectively. In studies using 4-nitrophenol as a model toxic compound, increasing 4-nitrophenol
19 concentrations resulted in an approximately equal decrease in current in all MFC in the MFC array (63%, 66% and 74%
20 respectively when exposed to medium containing 150 mg/L 4-nitrophenol). Thus the magnitude and ordering of the
21 response allowed a decrease in signal from decreasing BOD to be distinguished from the presence of a toxic compound.
22 Furthermore, the MFCs were capable of recovering to previous performance levels within hours of acute exposure to
23 toxicity. The multi-stage MFC configuration therefore enabled truly combined BOD and toxicity sensing with enhanced
24 detection capabilities without the need for a defined or synthetic reference feed.

25 Water impact

26 Online microbial fuel cell-based toxicity sensors could protect biological treatment plants by early detection of harmful toxic
27 influents without being selective to specific toxicants. Conventional MFC sensors cannot distinguish a decrease in signal caused by
28 toxicity from a decrease in BOD. Our multi-stage MFC-based sensor elegantly solves this problem, and offers definitive online
29 toxicity detection using bacteria enriched from wastewater.

31 1 Introduction

32 To ensure environmental and health security for downstream
33 water users real-time water quality monitoring is becoming a
34 necessity. Increasing water consumption worldwide and
35 incoming regulations such as those from the European Union,
36 and Indian Central Pollution Control Board², will drive demand
37 for real time monitoring technologies. Organic loading (e.g.
38 Biochemical Oxygen Demand; BOD) and toxicity are important
39 water quality parameters which are difficult to measure on line
40 and conventional measurement methods are labour-intensive

41 and time-consuming which prevents their use for real-time
42 monitoring.

43 The faradaic current or charge generated from a Microbial Fuel
Cell (MFC) coupled to consumption of labile organic carbon by
the anodic biofilm can be correlated to the concentration of
substrate consumed. This recent technological advance has led
to development of MFC-based sensors for detection of several
environmental factors^{3,4} including BOD, specific substrates,
dissolved oxygen and microbial activity.^{5–8} Conversely,
inhibition of the electrical current in MFCs (by external
influences) has enabled sensors for toxicity and specific heavy
metals.^{9,10}

53 MFCs have shown potential for application as low-cost, real-
time water quality sensors for estimation of BOD and toxicity
and offer the possibility of monitoring both parameters with a
single sensor.^{11–14} A major issue for combined monitoring
systems is that in order to accurately detect a change in one

^a School of Natural and Environmental Sciences, Newcastle University, Newcastle upon Tyne, NE1 7RU, UK.

^b School of Engineering, Newcastle University, Newcastle upon Tyne, NE1 7RU, UK.
* Email: Ian.Head@newcastle.ac.uk; Telephone: (+44)1912086605

Electronic Supplementary Information (ESI) available. See DOI: 10.1039/x0xx00000x

parameter (e.g. toxicity) the other is required to be fixed (e.g. BOD) and vice versa¹⁵. This has led to development of complex sensors which require frequent or parallel feeding with synthetic feeds (e.g. containing a known BOD concentration) to attribute response specifically to one or the other of the measured parameters, detracting from the low-cost and real-time monitoring benefits offered by MFC-based sensors. Stable detection of Cu(II) has been demonstrated in a system where BOD levels were artificially supplemented with glucose and acetate^{16,17}, however Tan et al.¹⁷ noted that this reduced bioavailable toxicant and thus reduced sensor sensitivity. We have reported previously that using multi-stage hydraulically-connected MFCs can extend the sensing range for organic material/BOD¹⁸. In the present study, we demonstrate an innovative approach to combined BOD and toxicity monitoring in a single sensor using multi-stage MFCs. This allowed explicit differentiation of signal decrease due to the presence of a toxic substance from signal decrease due a drop in organic load without requiring a separate reference feed with defined organic load or amendment with the toxic substance being measured.

2 Methods

2.1 Synthetic Wastewater Medium

The feed used to test the sensor was a phosphate buffered medium containing glucose and glutamic acid (GGA)¹⁸. This uses the same carbon source as the standard medium used to calibrate and test conventional BOD₅ assays¹⁹. In order to change the organic loading, the GGA concentration was varied between 100–2000 mg/L (60–1199 mg/L O₂ BOD₅). For toxicity tests, 10–150 mg/L 4-nitrophenol (4-NP; Sigma-Aldrich), as a model toxic compound, was added to 360 mg/L O₂ BOD₅ (600 mg/L GGA) medium before making up to the required volume with deionised water. 4-NP is commonly used as a model compound to test a range of toxicity assays²⁰.

2.2 Microbial Fuel Cells

10 mL single chamber MFCs were assembled with a carbon cloth anode (effective area (A_{Eff}) of exposed electrode not covered by gasket = 4.91 cm²), 0.5 mg/cm² Pt gas diffusion cathode and Fumapem F-930 cation exchange membrane (FuMA-Tech), operated with an external resistance (R_{Ext}) of 305 Ω . The cell voltages were recorded using a NI-USB 6225 datalogger and LabVIEW SignalExpress data acquisition software (National Instruments). The current was calculated from $I = V/R_{\text{Ext}}$ and current density by dividing by A_{Eff} .

2.3 Single-pass, continuous flow system

A three-stage array of MFCs was constructed in triplicate in the same configuration as described in detail in our previous study.¹⁸ Briefly, each feed line comprised a five-litre medium bottle containing up to 5600 mL synthetic wastewater medium (without 4-NP) leading to a sterile drip chamber, a peristaltic pump and then past a UV lamp (to minimise upstream contamination). Medium was pumped at maximum 1.24

mL/min into the three-stage MFC array and to a waste collection vessel in single-pass mode. In this study, three-way valves were installed upstream of the peristaltic pump (Figure S1, position 3-W M; ESI) to allow the medium feed to be switched to a feed with different BOD levels or containing toxicant, in order for the sensor response to acute BOD changes and toxic shock events to be tested. Valves were also installed downstream for sampling after the final MFC (Figure S1, 3-W 3; ESI).

2.4 Assessing inhibition due to very high BOD levels

The MFCs response to substrate inhibition was assessed as it is a well-known microbiological phenomenon involving the inhibition of bacteria at excessive substrate concentrations^{21–23}. To assess the effect at high levels of glucose and glutamic acid (e.g. 1199 mg/L O₂ BOD₅) the medium was changed from a low BOD concentration (e.g. 150–300 mg/L BOD₅) to a high BOD concentration using the procedure described in section 2.3.

2.5 Simulation of an acute toxic event

For testing of inhibition events due to the presence of a toxic chemical, the BOD₅ was maintained at 360 mg/L O₂ BOD₅ (600 mg/L GGA) in the five-litre medium bottle and events were simulated by switching the peristaltic pump inlet feed using the 3-W M valve (Figure S1, ESI) from the 5-litre bottle to a 500 mL bottle containing the toxic compound to be tested. Acute exposure tests were conducted with medium containing 4-NP pumped for 90 minutes before reconnecting the feed with no 4-NP present and monitoring the recovery of current generation. Experiments were conducted starting with the lowest concentration of 4-NP to ensure that the maximum data could be amassed in the event of total biofilm death due to exposure to the toxic compound. In all tests one of the replicate MFCs arrays (feed line B, Figure S1, feed line B ESI) was used as a control and the feed was not switched from the non-toxic 360 mg/L O₂ BOD₅ medium fed from the five litre bottle. The exact same procedure was used for testing the response to acute decreases in BOD from 500 mL bottles containing medium with different levels of BOD without 4-NP. It should be noted that feed B was used as a control for experimental purposes only and is not required to distinguish toxicity from a drop in BOD in this system.

2.6 Analytical Methods

BOD₅ tests were performed following the APHA standard procedure¹⁹. From four 1/250-diluted replicates of each sample, a single initial dissolved oxygen (DO) measurement and three final DO measurements were taken after incubation at 20 °C for 5 days. A conversion ratio of 0.599 BOD₅/GGA was measured and used to calculate BOD₅ values from known medium GGA concentrations.

Chemical Oxygen Demand (COD) was determined from samples digested at 148 °C with potassium dichromate for 2 hours using a photometric test kit according to the manufacturer's instructions. Absorbance values at 605 nm were measured

167 using a Spectroquant Pharo 300 spectrophotometer (Merck
168 Millipore).

169 4-nitrophenol was determined from samples adjusted to pH 3–
170 4 by addition of 4 μL HCl (35%) to 1 mL sample and measuring
171 its absorbance at 320 nm with a Spectrostar Nano
172 spectrophotometer (BMG Labtech) in comparison to a
173 calibration constructed using external standards.

174 2.7 Current Density Normalisation

176 The current density generated by each MFC was normalised to
177 100% to permit comparisons between cells irrespective of
178 electrochemical performance (i.e. caused by cathode
179 degradation¹⁸). For each medium cycle, the average stable
180 current density (\bar{I}) was determined as the average current
181 density during the period in which the first derivative (dI/dt ;
182 which approached zero as the current stabilised) was below 3%
183 of the peak current density. Normalised, average stable current
184 density ($\bar{I}/\bar{I}_{\text{Max}} \times 100\%$) was thus calculated from the maximum,
185 average stable current density (\bar{I}_{Max}). Limit of detection²⁴ was
186 calculated ($3.3 \times \text{SD}_{\text{Res}}/m$) from the residual standard deviation
187 (SD_{Res}) about fitted (current vs concentration) calibration lines
188 and the linear regression slope ($m = \text{sensitivity}^{11}$).

189 3 Theory

191 Current density sensing principles must be established in order
192 to identify water quality events based on the response of a MFC.
193 With MFC sensing an increase in current can be generally
194 attributed to increases in BOD, however it has been shown that
195 presence of respiratory inhibitors can result in an increase in
196 MFC current density when competing terminal electron
197 accepting compounds are also present (as only the electrode
198 can be utilised).²⁵ Prior to this study, an approach to distinguish
199 decreases in current caused by decreases in BOD from those
200 caused by the presence of toxic compounds without controlling
201 one of these parameters had not been established.

202 As with any biosensor, various environmental factors (e.g. non-
203 optimal pH or temperature, lower conductivity and higher
204 dissolved oxygen levels) can also result in changes in the
205 response (e.g. MFC current) which are not associated with the
206 target analytes (e.g. BOD or toxicity). Yet these parameters are
207 readily measured online using conventional electrochemical
208 probes and can therefore be accounted for in calibration
209 models.

210 Under typical operation of a three-stage MFC-based BOD sensor
211 with non-toxic media, current generation was observed initially
212 in the first-stage MFC¹⁸. This was followed by the second and
213 third-stage MFCs as BOD was increased, the first-stage biofilm
214 saturated and maximum current was reached; delivering a
215 partially-degraded effluent to the downstream MFCs (Figure
216 1a/b/c). It is this ordered response which proffers opportunities
217 for sensing applications.

218

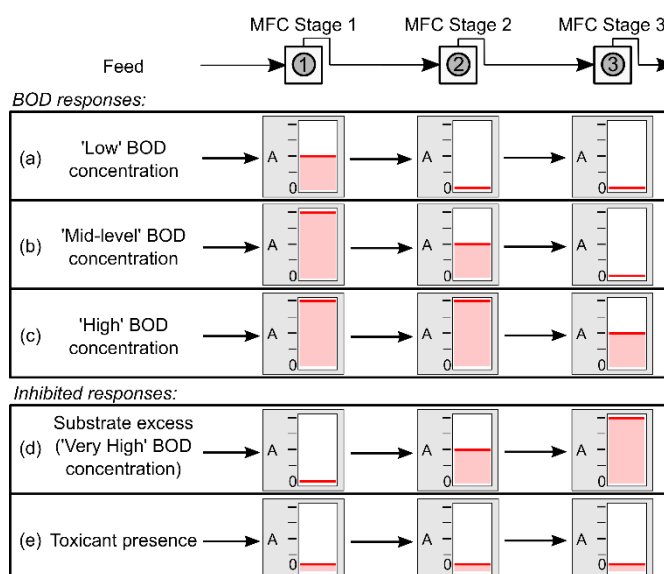


Figure 1: Schematic diagram of scenarios regarding BOD sensing and inhibition leading to decreases in current to be addressed with multi-stage MFCs. Examples are given for (a) 'low', (b) 'mid-level' and (c) 'high' BOD concentrations and inhibition events of (d) substrate excess and (e) toxicant presence. The relative, hypothesised electrical current (– in amperes (A)) response is indicated for each MFC in a three-stage hydraulic array.

219 3.1 Current response to increases in BOD

220 As BOD concentrations in a feed to a multi-stage MFC increase
221 to levels above which the anodic biofilms can operate
222 maximally, current decrease has been observed due to
223 inhibition caused by substrate excess.^{18,23} Here, the substrate
224 acts as a biodegradable toxicant and inhibits electrogenic
225 activity by anodic bacteria. As the first stage MFCs receive the
226 highest dose of medium they would be expected to respond (be
227 inhibited) the most. When substrate is consumed non-
228 electrogenically (fermented) in the upstream MFCs, the BOD
229 level would decrease to non-inhibitory levels and thus less
230 inhibition would be expected in the downstream MFCs. If the
231 downstream MFCs were not saturated they would exhibit a
232 current increase due to increased levels of BOD in the feed
233 received. The current output observed during substrate excess
234 events could therefore be characterised by current in stage 1 <
235 stage 2 < stage 3 (Figure 1d).

236 3.2 Current response to decreases in BOD

237 Decreases in BOD of a feed to a multi-stage MFC configuration
238 result in an ordered decrease in current with the initial and
239 greatest current decrease observed in the final stage MFC
240 (Figure 1c to 1b to 1a) i.e. current decrease in the order 3 > 2 >
241 1. This is likely because the third-stage cell 'starves' first as it
242 receives the degraded effluent of the second and first-stage
243 MFCs. Therefore, once BOD is lowered below the saturation
244 concentration of the second and first stage MFCs, the current
245 decreases in those cells as well (Figure 1b to 1a).

246

247

248

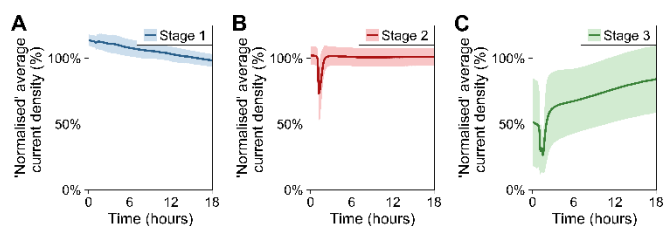


Figure 2: Average normalised current density response of the (a) first, (b) second and (c) third stages of MFCs to a BOD increase from 300 (0-1 hour) to 360 (1-18 hour) mg/L O₂ BOD₅ (estimated from GGA concentration) showing saturation in stages 1 and 2 and an increase in current in the third stage MFC. The inflection point at approximately 1 hour was when the medium replacement occurred. Shaded bands are \pm SD from triplicate cells.

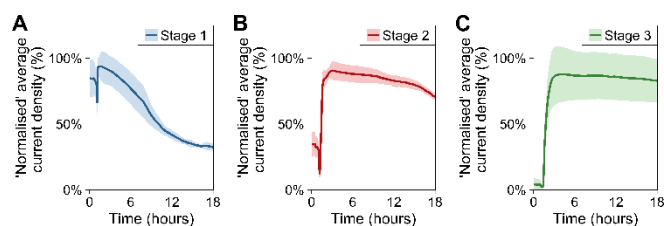


Figure 3: Average normalised current density response of the (a) first, (b) second and (c) third stages of flow-mode MFCs to a BOD increase (medium bottle replacement) from 150 (0-1 hour) to 1199 (1-18 hour) mg/L O₂ BOD₅ (estimated from GGA concentration) showing current decrease in first stage response. The inflection point at approximately 1 hour was when the medium replacement occurred. Shaded bands are \pm SD from triplicate cells.

249 3.3 Presence of toxic compounds

250 When a toxic compound is present in the feed, the first-stage
251 MFCs would receive the highest dose. However, for non-readily
252 biodegradable toxicants no consumption would occur and the
253 toxicant concentration would not decrease between the first
254 and the final MFC. Consequently, the downstream MFCs would
255 be expected to be inhibited to the same degree, resulting in a
256 decrease in current more or less simultaneously, depending on
257 the hydraulic retention time, in all MFCs in the hydraulically
258 connected array. Inhibition caused by a non-biodegradable
259 toxicant could therefore be identified by approximately equal
260 decrease in current in each MFC, i.e. 1=2=3 (Figure 1e).
261 Thus, the pattern of signal output from the three stages of the
262 sensor distinguishes different types of toxicity event from a
263 decrease in BOD (Figure 1d/e vs Figure 1c-b-a).

264 4 Results and discussion

265 4.1 Microbial Fuel Cell setup and operation

266 All MFCs were set up in a triplicate three-stage hydraulic array
267 (Figure S1, ESI) and were inoculated on day 0 with effluent from
268 batch-fed MFCs, initially inoculated with activated sludge from
269 a wastewater treatment plant (Tudhoe Mill, Northumbria
270 Water Ltd). Following a 14-day batch-mode enrichment MFCs
271 achieved peak current densities of 246.7 ± 12.3 , 245.4 ± 21.6
272 and $265.7 \pm 11.1 \mu\text{A}/\text{cm}^2$ in the first, second and third stages
273 respectively. At this time operation was switched from batch to
274 continuous single-pass operation fed from sterile medium
275 bottles. The experiments reported here were conducted
276 following 126 days of operation with GGA medium (not
277 containing any toxicants). During this 126 days of operation the
278 sensor was tested for its ability to measure BOD₅ at higher
279 concentrations than a single-stage sensor¹⁸. Following this
280 initial development of the sensor for BOD measurement we
281 tested its utility as a toxicity sensor. The ability to operate the
282 sensor for toxicity detection is reported here.

284 4.2 Multi-stage MFCs response to BOD increases

285 With a step-up change in BOD₅ from 300 to 360 mg/L the first
286 and second stage MFCs were observed to remain at
287 approximately 100% of the normalised current density (Figure
288 2A, 2B; 0-1 hour = 300 mg/L, 1-18 hour = 360 mg/L). The
289 response of the third stage MFCs increased from 54% (\pm 37%)

290 with 300 mg/L O₂ BOD₅ to 76% (\pm 24%) normalised current
291 density with 360 mg/L O₂ BOD₅ (Figure 2C). The greatest degree
292 of variability was observed with unsaturated MFCs (operating at
293 BOD concentrations below levels that gave maximum MFC
294 output). This could be attributed to replicate MFCs having small
295 performance differences and larger relative variation with
296 respect to low absolute values of output from the cells.
297 Performance differences may have arisen during preparation
298 (i.e. cathode ink application affecting MFC performance) or due
299 to small flow rate differences (i.e. flow rate was measured as
300 1.09-1.24 ml/min) across channels A-C.

A feed concentration of 360 mg/L O₂ BOD₅ was chosen as a
301 starting condition for current decrease tests (section 4.4 and
302 4.5). Preliminary tests determined that it was sufficient to
303 saturate the first and second stage MFCs and give capacity in
304 the third stage MFCs to increase or decrease current output
305 based on inhibition and starvation treatments (Figure 2).

307 4.3 Multi-stage MFCs response to substrate inhibition at high BOD

308 The current density of the three-stage MFCs was also assessed
309 in response to a medium concentration step-up change from
150 to 1199 mg/L O₂ BOD₅ (250 to 2000 mg/L GGA; Figure 3).
310 At the starting BOD₅ of 150 mg/L O₂, the first stage MFCs were
311 close to the upper limit of linearity and were almost saturated
312 with an average normalised current density of 85% (\pm 8%). The
313 second and third MFC stages were not saturated at this
314 concentration and had average normalised current densities of
315 36% (\pm 10%) and 4% (\pm 4%) respectively.

316 The upper limits of linear response for each stage had been
317 previously determined (as 180, 300 and 420 mg/L O₂ BOD₅
318 respectively; Figure S2, ESI). It was therefore reasoned that
319 medium containing 1199 mg/L O₂ BOD₅, would be in excess of
320 the capacity of each MFC individually or all three combined and
321 would be expected to output the maximum current density at
322 this concentration (100%). Immediately after medium
323 replacement the normalised current densities in each stage
324 were observed to increase close to 100% (Figure 3). However,
325 despite the increase in concentration, a steady decrease in
326 normalised current density was observed in the first stage MFCs
327 to 32% (\pm 2%) (Figure 3A, 18h). The normalised current density
328 in the second stage of MFCs fell to 68% (\pm 4%) (Figure 3B, 18h)
329 and the third stage MFCs remained at a normalised current
330 density of 83% (\pm 13%) (Figure 3C, 18h).

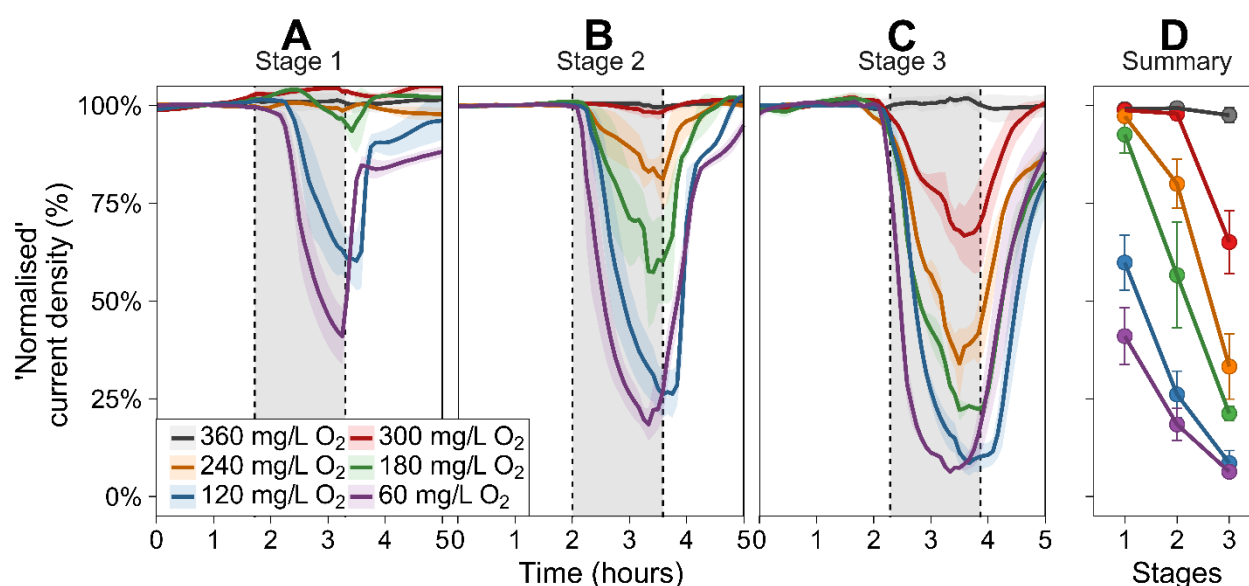


Figure 4: Normalised average current density response of three stages of MFCs to decreases in BOD₅ from 360 to 60 mg/L O₂ (estimated from GGA concentration). The dashed line-enclosed region is the period during which the low-BOD medium was fed to MFCs and current decreases were observed. Coloured, shaded bands and error bars are the range of values from duplicate MFCs in flow channels A and C (channel B is black control fed 360 mg/L O₂ BOD₅). Summary plot shows minima values from each current decrease test cycle at each MFC stage.

334 The trend in normalised current densities (32% < 68% < 83%)
 335 showed an increase down the hydraulic series which was
 336 concurrent with the theoretical prediction (Section 3.2, Figure
 337 1d) with current in stage 1 < stage 2 < stage 3 (Figure 1d). This
 338 behaviour of the three-stage MFCs suggested that substrate
 339 inhibition occurred in the upstream MFCs but due to the
 340 biodegradability of the substrate, sufficient substrate had been
 341 removed to reduce the degree of inhibition in the downstream
 342 MFCs.

344 4.4 Multi-stage MFCs response to BOD decreases

345 The response of the multi-stage MFCs to decreases in BOD was
 346 systematically assessed by diverting the medium feed using the
 347 3-W M three-way valve (Figure S1, ESI) from a 360 mg/L O₂ BOD₅
 348 medium bottle to a solution of lower BOD concentration. Five
 349 lower BOD₅ solutions were tested, each over a 90 minute
 350 period, before switching back to a 360 mg/L O₂ feed (Figure 4).
 351 With a 300 mg/L O₂ (Δ60 mg/L O₂) BOD₅ medium, no loss of
 352 response was observed in the first and second stages of MFCs
 353 (i.e. remained at 100% (±2%)) (Figure 4A and B). The third stage
 354 MFCs normalised current density decreased to 65% (±8%)
 355 (Figure 4C). As the BOD₅ concentration was lowered further,
 356 greater decreases in current density were observed with the
 357 third followed by the second and first stage MFCs. When
 358 medium containing 60 mg/L O₂ (Δ300 mg/L O₂) BOD₅ was
 359 passed through the cells the normalised current density in the
 360 first, second and third stage MFCs was reduced by 59% (±7%),
 361 82% (±4%) and 94% (±0%) respectively. The limit of detection
 362 for changes in BOD₅ was a difference of 43.7, 55.5 and 59.6
 363 mg/L in the first, second and third stage MFCs respectively and

the average sensitivity was 0.4% of the normalised current
 density per mg/L change in BOD₅.

The trend observed (shown by the Summary plot in Figure 4D),
 followed the same order as step-up BOD increases due to the
 first stage MFCs receiving the highest concentration of
 substrate, followed by the second and then third stages of
 MFCs. Thus the third stages responded first ('starved' first)
 as they were fed last. The trend in current decrease (e.g. 59% <
 82% < 94% lost) showed greater decrease in output down the
 hydraulic series which was concurrent with the predicted order
 hypothesised earlier (output stage 3 < 2 < 1; Figure 1c-b-a). A
 calibration curve fitted to the Hill equation was produced by
 transforming the current density to current density loss (%) and
 the medium BOD₅ to the change in BOD₅ (ΔBOD₅; Figure S3, ESI).
 The BOD decrease current loss calibration was a reflection of
 the response observed with current generation.¹⁸ With current
 loss (due to BOD decrease), the third stage MFCs responded
 first as the smallest decreases resulted in those cells receiving
 the least substrate.

4.4.1 Analysis of effluent from MFCs during BOD decrease events

Immediately following the restoration of the 360 mg/L O₂ BOD₅
 feed samples were taken from each flow channel at the 3-W 3
 three-way sampling valve (Figure S1, ESI). The flow path took 59
 minutes at 1.24 mL/min to reach the 3-W 3 valves (passing
 through the first, second and third MFC stages), therefore after
 90 minutes of testing low BOD solutions the effluent would have
 been flowing past this sampling point for 45 minutes. Samples
 were also taken of the fresh low-BOD medium prior to feeding to
 the MFCs (Figure 5).

394 With a decrease to 60 mg/L O₂ BOD₅ (102 mg/L O₂ COD), the
 395 effluent COD of the flow channels A and C was observed to
 396 decrease by 84 ±5%. The effluent COD reduced from 115 ±12
 397 mg/L O₂ COD and 90 ±10 mg/L O₂ COD down to 24 ±1 mg/L O₂
 398 COD and 19 ±7 mg/L O₂ COD in channels A and C respectively.
 399 The effluent from flow channel B, which was maintained as a
 400 control at a constant BOD₅ of 360 mg/L O₂ (613 mg/L O₂ COD),
 401 was quite variable between samples but remained
 402 approximately constant at 91 ±23 mg/L O₂ COD averaged over
 403 all treatments (Figure 5, inset).

404 Analysis of the effluent samples confirmed that the COD
 405 concentration was significantly lower in the outlet than the
 406 fresh medium bottle and therefore validated the theory that
 407 with decreases in feed BOD, the concentration of substrate
 408 received at the third stage of MFCs was less than in stage 1 and
 409 2 as biodegradable substrate decreased through the hydraulic
 410 array. This led to the observed order in current decreases as the
 411 third stages of MFCs became depleted of substrate (starved)
 412 first and thus generated the least current (see Figure 1c-b-a).

4.5 Multi-stage MFCs response to toxicant presence

414 The response of the multi-stage MFCs to toxicant exposure was
 415 assessed with 4-nitrophenol (4-NP) present in the anolyte feed.
 416 The same method as testing BOD decreases was employed. Five
 417 toxicant-doped medium solutions were tested each over a 90
 418 minute period each before switching back to a 360 mg/L O₂ feed
 419 to enable biofilm recovery (Figure 7).

420 No loss in current response was detectable with 4-NP
 421 concentrations of 10 and 25 mg/L in the three-stage MFCs.
 422 As the 4-NP concentration was increased to 75 mg/L and above
 423 in subsequent cycles, decreases in current density were
 424 observed in all MFC stages. When a 150 mg/L 4-NP-doped
 425 medium was passed through the normalised current densities
 426 of cells in the first, second and third stage MFCs were reduced
 427 to 37% (±29%), 34% (±15%) and 26% (±6%) respectively. There
 428 was no ordered trend observed along the hydraulic series
 429 (shown by approximately equal current decreases (inhibition)
 430 each MFC stage in the Summary plot in Figure 7D). Thus, the

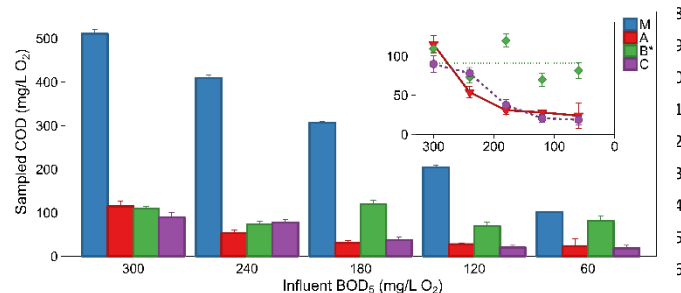


Figure 6: COD measured at each sampling point after 90 minutes of BOD decrease from 360 mg/L O₂ BOD₅ (estimated from GGA concentration; M = Fresh medium sample; A, B & C = Final effluents from 3-W 3 valve in each flow channel). Inset shows COD of effluents from each channel in a line graph. Error bars are the range from duplicate measurements. *Channel B was maintained at 360 mg/L O₂ BOD₅ as a control.

431 decrease in current density response was distinct from BOD
 432 related current decreases (both substrate excess inhibition and
 433 BOD decreases).

The limit of detection was 67.1, 89.6 and 76.4 mg/L 4-NP in the first, second and third stage MFCs and the average sensitivity was 0.5% of the normalised current density per mg/L 4-NP.

This observation suggested that the toxicant was not consumed within the MFCs and each stage received approximately the same dose of toxicant, resulting in the same degree of inhibition (as hypothesised for non-/slowly-biodegradable toxicants (see Figure 1e).

After the non-toxic medium was restored, the current density recovery following the 150 mg/L 4-NP toxic exposure was monitored (Figure S4, ESI). 11.5 hours after the 360 mg/L BOD₅ medium feed had been restored, the inhibited MFCs recovered to the same normalised current density as the control MFC (in

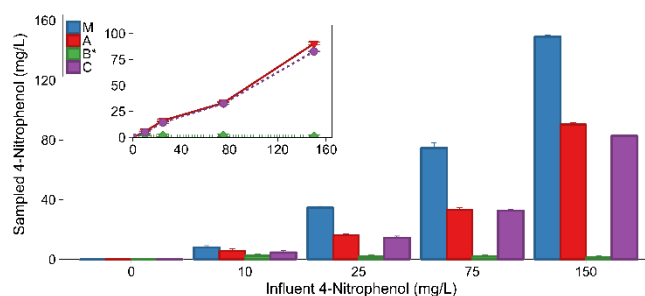


Figure 5: 4-Nitrophenol (4-NP) concentrations measured at each sampling point after 90 minutes of toxicant exposure (M = Fresh medium sample; A, B & C = Final effluents from 3-W 3 valve in each flow channel). Inset shows effluents from each channel in a line graph. Error bars are the range from duplicate measurements. *Channel B was maintained with no 4-NP as a control.

flow channel B). This recovery period was much greater than the recovery times of up to four hours observed for the exposure tests with 4-NP concentrations below 112.5 mg/L (Table S1, ESI). Kim et al.²⁶ also observed increased recovery times following increased levels of toxicity (up to 8 hours following a 1 mg/L cadmium dosing). Additionally, this long response time was only observed with the first stage MFCs, this mirrors the recovery response following exposure to inhibitory substrate concentrations but in reverse order compared to the BOD decrease response (with low BOD the stage 3 MFC which is most 'starved' takes longest to recover). The fact the biofilm completely recovered to pre-toxic current density showed the resilience of the MFC-based sensor.

4.5.1 Analysis of Effluent from MFCs Exposed to 4-Nitrophenol

Samples were taken from the 3-W 3 valve (Figure S1, ESI) in each channel immediately following the restoration of the non-inhibitory GGA feed (360 mg/L O₂ BOD₅). Samples were also taken of the fresh 4-NP-doped medium prior to feeding to the MFCs (Figure 6).

The effluent 4-NP concentration of flow channels A and C was observed to decrease compared to the initial 4-NP-doped medium concentrations of up to 150 mg/L 4-NP. The 4-NP concentrations in effluents from channels A and C decreased on average by 47 ± 10% (Figure 6). The effluent from flow channel B, which was maintained as a control at a constant BOD₅ of 360 mg/L O₂ and no 4-NP, showed no absorption at 320 nm indicating that the values obtained for channels A and C could be attributed to 4-NP presence.

Analysis of 4-NP showed that there was a decrease in 4-NP concentration through the hydraulic array of MFCs. 4-

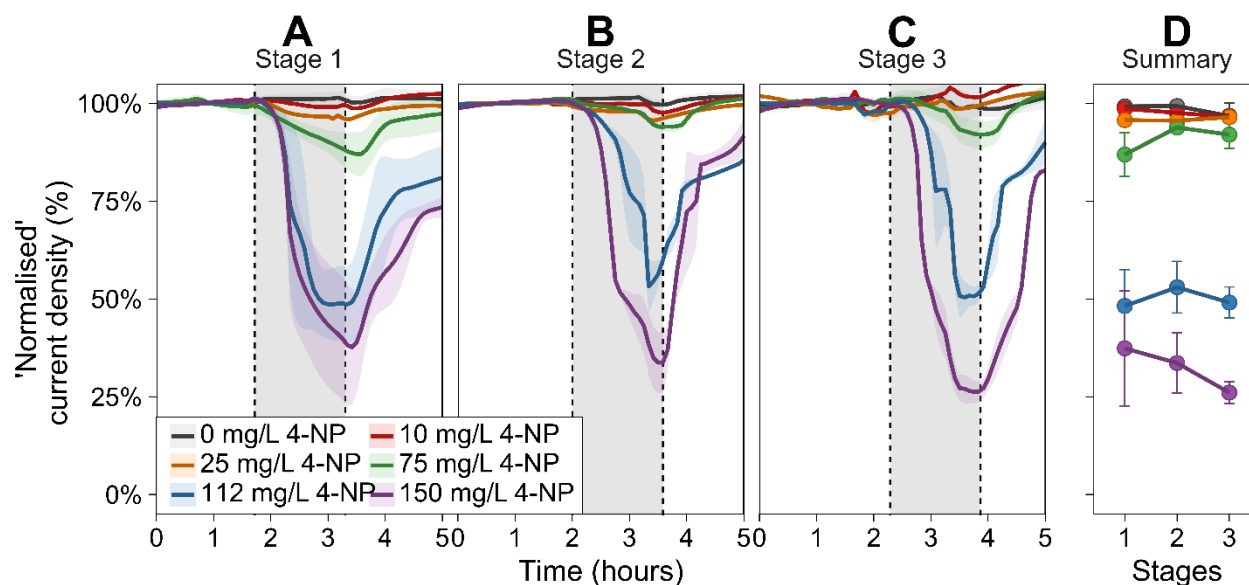


Figure 7: Normalised average current density response of three stages of MFCs to increasing concentrations of 4-nitrophenol (4-NP) from 0 to 150 mg/L. The shaded region enclosed by dashed lines is the period during which the toxicant-doped medium was fed to MFCs and current decreases were observed. Coloured, shaded bands and error bars are the range of values from duplicate MFCs in flow channels A and C (channel B is black control fed 0 mg/L 4-NP). Summary plot shows minima values from each current decrease test cycle at each MFC

477 nitrophenol is biodegradable in aerobic environments by
 478 bacteria which are able to completely convert 4-NP to carbon
 479 dioxide and water using the carbon and nitrogen for growth.^{27,11}
 480 Bacteria and archaea in anaerobic methanogenic bioreactors
 481 that have previously exposed to 4-NP for long periods, showed
 482 degradation of up to 100 mg/L 4-NP after days to weeks of
 483 exposure.²⁸ However, the tests in the present study were
 484 conducted over the course of 90 minutes which was not
 485 expected to be enough time to select for 4-NP-degrading
 486 bacteria (by the time the feed had reached the 3-W 3 valve and
 487 sampling was performed after only 45 minutes of exposure had
 488 elapsed).

489 It is therefore thought that the decrease in 4-NP occurred due
 490 to non-biological processes such as dilution due to the hydraulic
 491 retention time (HRT), adsorption within the hydraulic array or
 492 the 4-NP may have been reduced to 4-aminophenol under
 493 anoxic condition²⁹. When the 4-NP reached each 10 mL MFC
 494 chamber it is possible that the toxicant may have become mixed
 495 with non-toxic medium and thus diluted. With the HRT to reach
 496 the 3-W 3 valve approximately 45 minutes, and only 90 minutes
 497 toxicity tests being conducted (for operational and biofilm
 498 recovery reasons), it is likely that steady-state mixing and
 499 equilibration of the toxic medium across the hydraulic array had
 500 not occurred at the time of sampling (at least 3HRT = 135
 501 minutes would theoretically be required to ensure complete
 502 mixing). 4-NP persisting for longer within the hydraulic array
 503 would explain the prolonged recovery time of the MFCs with
 504 high concentrations of 4-NP. The observed current response of
 505 the MFCs did not appear to show that the 4-NP was being
 506 consumed/degraded, as an equal degree of inhibition was
 507 observed in each stage. For toxicants which are degraded as
 508 medium passed through the hydraulic array the response would

be expected to be similar to the substrate excess where the first stage MFCs receive the greatest dose. Further investigations, including lengthier exposure periods and sampling after each stage of MFCs would be required to confirm the fate of 4-NP in the MFC-based sensor.

5 Conclusions

MFC-based sensors for measurement of organic load or toxic materials in wastewater are hampered by the inability to distinguish a decrease in current caused by a decrease in organic load from a decrease caused by the presence of a toxic material. If such a sensor was used for process control, the consequences of mischaracterising BOD and toxicity related incidents would be severe. Low BOD indicates that treatment process parameters (e.g. aeration rate) can be reduced, whereas high BOD effluents containing toxicants would require prompt notification of operators that higher levels of treatment are required or possibly intervention to protect the micro-organisms in biological treatment processes.

We have devised an MFC biosensor configuration that allows these two situations to be distinguished and furthermore distinguish substrate inhibition from inhibition caused by a poorly, or non-biodegradable toxicant. While the system hydraulic retention time (HRT) (from inlet of MFC1 to outlet of MFC3) is increased by having three MFCs hydraulically in series, the individual HRT of each cell is not impacted and thus the sensitivity and responsiveness remains the same as single-stage MFCs as the current from each cell is monitored individually. If one considers that stage 1 MFCs behave exactly as a conventional single stage MFC-based sensor (Figure 8, top row only), there is no way to differentiate decreased current density

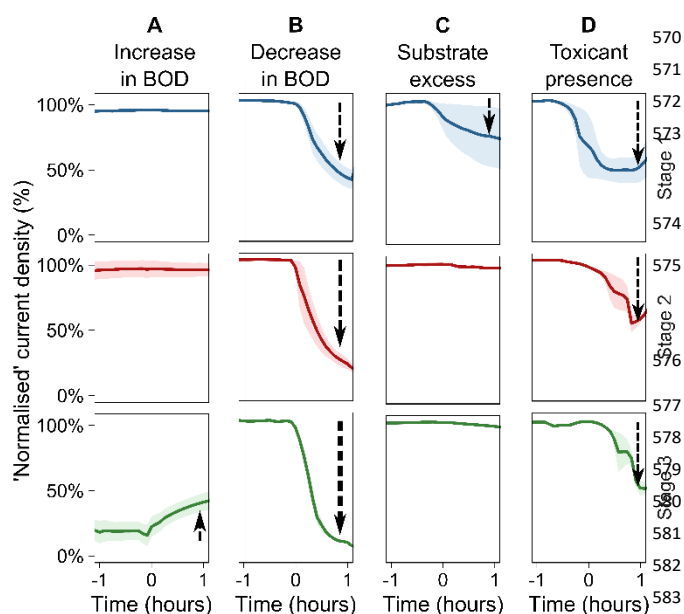


Figure 8: Representative examples of the average current densities (shaded region is \pm SD) obtained from multi-stage MFCs to scenarios which would not be distinguishable with single-stage MFCs (i.e. row 1 only). (A) BOD increase can be detected by response of third stage MFCs (which are not at 100% saturation). It is also possible to distinguish between decreases in current density due to (B) BOD decrease (current decreases in stage 3 > 2 > 1 order), (C) substrate excess (current decreases in 1 > 2 > 3 order) and (D) toxicant (4-NP) presence (equal current decreases in all stages). $t = 0$ is the approximate point at which the event occurred.

caused by BOD decrease (Figure 8B) substrate excess (Figure 8C) or toxicant presence (Figure 8D). The multi-stage MFCs however exhibited an ordered response, which can be used to explicitly differentiate these three different types of event.

- Decreases in BOD_5 led to a decrease in current density with downstream (third stage) MFCs receiving the lowest concentration of substrate and therefore 'starved' first (confirmed by COD measurements) (Figure 8A).
- Increases in BOD_5 to excessive levels of substrate (e.g. 1199 mg/L O_2) resulted in inhibition and loss of current in upstream MFCs first as the 'strongest dose' was received there (Figure 8B).
- With 4-NP toxicant presence no ordered response was observed, with each stage of MFC being equally inhibited by the toxicant as the medium passed through the hydraulic array (Figure 8C).

MFC-based toxicity sensors were shown to be capable of full recovery to pre-toxic current densities, however recovery from highly toxic 'shock' events could take considerable time (e.g. 11.5 hours following a 150 mg/L 4-NP dosing) to recover to 100% normalised current density. We have a reported an innovative method for distinguishing toxicity and BOD-related responses using a MFC-based sensing system. Based on the ordered responses observed in the presence of a toxic substance (first stage MFC responds first) or with a change in BOD (last-stage MFC responds first) these different types of event are distinguishable using this framework. Nevertheless an important limitation is that the sensor would not be able to determine the presence of a toxicant under very low BOD conditions, as at low BOD there would be minimal electrical

output from the sensor. The presence of acute toxicity presence during an acute change in BOD could also lead to complex outputs from the sensor that would require further systematic testing to resolve.

Conflicts of interest

There are no conflicts to declare.

Acknowledgements

This research was funded by the EPSRC Supergen Biological Fuel Cells (EP/H019480/1) and our research on bioelectrochemical systems for sensing applications has been supported by BBSRC (BB/P000312/1, BIV2017003, BB/R005613/1), EPSRC (EP/R511584/1), NERC (NE/L01422X/1) and Newcastle University Institute for Sustainability. Data supporting this publication is openly available under an 'Open Data Commons Open Database License'. Additional metadata are available at: <http://dx.doi.org/10.17634/154300-94>.

Notes and references

- (1) European Commission. *Directive 2000/60/EC of the European Parliament and of the Council of 23 October 2000 Establishing a Framework for Community Action in the Field of Water Policy*; 2000; Vol. L327, pp 1–82. <https://doi.org/10.1039/ap9842100196>.
- (2) Indian Central Pollution Control Board. *Directions Under Section 18(1)(B) Of The Water (Prevention & Control Of Pollution) Act, 1974 And The Air (Prevention & Control Of Pollution) Act, 1981 In The Matter Of Pollution Control*; India, 2014; p 10.
- (3) Abrevaya, X. C.; Sacco, N. J.; Bonetto, M. C.; Hilding-Ohlsson, A.; Cortón, E. Analytical Applications of Microbial Fuel Cells. Part I: Biochemical Oxygen Demand. *Biosens. Bioelectron.* **2015**, *63C*, 580–590. <https://doi.org/10.1016/j.bios.2014.04.034>.
- (4) Abrevaya, X. C.; Sacco, N. J.; Bonetto, M. C.; Hilding-Ohlsson, A.; Cortón, E. Analytical Applications of Microbial Fuel Cells. Part II: Toxicity, Microbial Activity and Quantification, Single Analyte Detection and Other Uses. *Biosens. Bioelectron.* **2015**, *63C*, 591–601. <https://doi.org/10.1016/j.bios.2014.04.053>.
- (5) Kim, B. H.; Chang, I. S.; Gil, G. C.; Park, H. S.; Kim, H. J. Novel BOD (Biological Oxygen Demand) Sensor Using Mediator-Less Microbial Fuel Cell. *Biotechnol. Lett.* **2003**, *25* (7), 541–545.
- (6) Liu, Z.; Liu, J.; Zhang, S.; Xing, X.-H.; Su, Z. Microbial Fuel Cell Based Biosensor for in Situ Monitoring of Anaerobic Digestion Process. *Bioresour. Technol.* **2011**, *102* (22), 10221–10229. <https://doi.org/10.1016/j.biortech.2011.08.053>.
- (7) Zhang, Y.; Angelidaki, I. A Simple and Rapid Method for Monitoring Dissolved Oxygen in Water with a Submersible

- 620 Microbial Fuel Cell (SBMFC). *Biosens. Bioelectron.* **2012**, *38*,
621 (1), 189–194. <https://doi.org/10.1016/j.bios.2012.05.032> (18)
- 622 (8) Tront, J. M.; Fortner, J. D.; Plötze, M.; Hughes, J. B.; Puzir,
623 A. M. Microbial Fuel Cell Biosensor for in Situ Assessment
624 of Microbial Activity. *Biosens. Bioelectron.* **2008**, *24* (4),
625 586–590. <https://doi.org/10.1016/j.bios.2008.06.006>. 678
- 626 (9) Patil, S.; Harnisch, F.; Schroder, U. Toxicity Response of
627 Electroactive Microbial Biofilms - a Decisive Feature for
628 Potential Biosensor and Power Source Applications. *ChemPhysChem* **2010**, *11* (13), 2834–2837. 681
629 <https://doi.org/10.1002/cphc.201000218>. 682
- 630 (10) Shen, Y.; Wang, M.; Chang, I. S.; Ng, H. Y. Effect of Shear
631 Rate on the Response of Microbial Fuel Cell Toxicity Sens
632 to Cu(II). *Bioresour. Technol.* **2013**, *136*, 707–710. 686
633 <https://doi.org/10.1016/j.biortech.2013.02.069>. 687 (21)
- 634 (11) Di Lorenzo, M.; Thomson, A. R.; Schneider, K.; Cameron, R.
635 J.; Ieropoulos, I. A Small-Scale Air-Cathode Microbial Fuel
636 Cell for on-Line Monitoring of Water Quality. *Biosens.*
637 *Bioelectron.* **2014**, *62*, 182–188. 691 (22)
638 <https://doi.org/10.1016/j.bios.2014.06.050>. 692
- 639 (12) Kim, M.; Park, H. S.; Jin, G. J.; Cho, W. H.; Lee, D. K.; Hyun,
640 M. S.; Choi, C. H.; Kim, H. J. A Novel Combined
641 Biomonitoring System for BOD Measurement and Toxicity
642 Detection Using Microbial Fuel Cells. In *5th IEEE Conference*
643 *on Sensors*; IEEE, 2006; Vol. 1–3, pp 1251–1252. 697 (23)
- 644 (13) Stein, N. E.; Hamelers, H. V. M.; Buisman, C. N. J. Stabilizing
645 the Baseline Current of a Microbial Fuel Cell-Based
646 Biosensor through Overpotential Control under Non-Toxic
647 Conditions. *Bioelectrochemistry* **2010**, *78* (1), 87–91. 701 (24)
648 <https://doi.org/DOI 10.1016/j.bioelechem.2009.09.009>. 702
- 649 (14) Xu, Z.; Liu, Y.; Williams, I.; Qian, F.; Li, Y.; Zhang, H.; Cai, D.
650 Wang, L.; Li, B. Disposable Self-Support Paper-Based Multi-
651 Anode Microbial Fuel Cell (PMMFC) Integrated with Power
652 Management System (PMS) as the Real Time “Shock”
653 Biosensor for Wastewater. *Biosens. Bioelectron.* **2016**, *85*,
654 232–239. <https://doi.org/10.1016/j.bios.2016.05.018>. 708
- 655 (15) Jiang, Y.; Liang, P.; Liu, P.; Bian, Y.; Miao, B.; Sun, X.; Zhang,
656 H.; Huang, X. Enhancing Signal Output and Avoiding
657 BOD/Toxicity Combined Shock Interference by Operating a
658 Microbial Fuel Cell Sensor with an Optimized Background
659 Concentration of Organic Matter. *Int. J. Mol. Sci.* **2016**, *17*,
660 1392. <https://doi.org/10.3390/ijms17091392>. 714 (27)
- 661 (16) Jiang, Y.; Liang, P.; Zhang, C.; Bian, Y.; Yang, X.; Huang, X.;
662 Girguis, P. R. Enhancing the Response of Microbial Fuel Cell
663 Based Toxicity Sensors to Cu(II) with the Applying of Flow
664 through Electrodes and Controlled Anode Potentials. *Bioresour. Technol.* **2015**, *190*, 367–372. 719
665 <https://doi.org/10.1016/j.biortech.2015.04.127>. 720
- 666 (17) Tan, Y. C.; Kharkwal, S.; Chew, K. K. W.; Alwi, R.; Mak, S. F.
667 W.; Ng, H. Y. Enhancing the Robustness of Microbial Fuel
668 Cell Sensor for Continuous Copper(II) Detection against
669 Organic Strength Fluctuations by Acetate and Glucose
670 Addition. *Bioresour. Technol.* **2018**, *259* (January), 357–
671 364. <https://doi.org/10.1016/j.biortech.2018.03.068>.
672 Spurr, M. W.; Yu, E. H.; Scott, K.; Head, I. M. Extending the
Dynamic Range of Biochemical Oxygen Demand Sensing
with Multi-Stage Microbial Fuel Cells. *Environ. Sci. Water
Res. Technol.* **2018**, *4* (12), 2029–2040.
<https://doi.org/10.1039/C8EW00497H>.
APHA. Biochemical Oxygen Demand (BOD). In *Standard
Methods for the Examination of Water and Wastewater*;
Clesceri, L. S., Greenberg, A. E., Eaton, A. D., Eds.; American
Public Health Association: Washington, DC, 1999; pp 1–12.
Nyholm, N.; Lindgaard-Jørgensen, P.; Hansen, N.
Biodegradation of 4-Nitrophenol in Standardized Aquatic
Degradation Tests. *Ecotoxicol. Environ. Saf.* **1984**, *8* (5),
451–470. [https://doi.org/10.1016/0147-6513\(84\)90066-6](https://doi.org/10.1016/0147-6513(84)90066-6).
Edwards, V. H. The Influence of High Substrate
Concentrations on Microbial Kinetics. *Biotechnol. Bioeng.*
1970, *12* (5), 679–712.
<https://doi.org/10.1002/bit.260120504>.
Borole, A. P.; Hamilton, C. Y.; Schell, D. J. Conversion of
Residual Organics in Corn Stover-Derived Biorefinery
Stream to Bioenergy via a Microbial Fuel Cell. *Environ. Sci.
Technol.* **2013**, *47* (1), 642–648.
<https://doi.org/10.1021/es3023495>.
Kong, X.; Yang, G.; Sun, Y. Performance Investigation of
Batch Mode Microbial Fuel Cells Fed With High
Concentration of Glucose. *Biomed. J. Sci. Tech. Res.* **2018**, *3*
(2), 122306.
<https://doi.org/10.26717/BJSTR.2018.03.000864>.
Shrivastava, A.; Gupta, V. Methods for the Determination
of Limit of Detection and Limit of Quantitation of the
Analytical Methods. *Chronicles Young Sci.* **2011**, *2* (1), 21–
25. <https://doi.org/10.4103/2229-5186.79345>.
Chang, I. S.; Moon, H.; Jang, J. K.; Kim, B. H. Improvement
of a Microbial Fuel Cell Performance as a BOD Sensor Using
Respiratory Inhibitors. *Biosens. Bioelectron.* **2005**, *20* (9),
1856–1859. [https://doi.org/DOI
10.1016/j.bios.2004.06.003](https://doi.org/DOI 10.1016/j.bios.2004.06.003).
Kim, M.; Hyun, M. S.; Gadd, G. M.; Kim, H. J. A Novel
Biomonitoring System Using Microbial Fuel Cells. *J. Environ.
Monit.* **2007**, *9* (12), 1323–1328. [https://doi.org/Doi
10.1039/B713114c](https://doi.org/Doi 10.1039/B713114c).
Samuel, M. S.; Sivaramakrishna, A.; Mehta, A.
Bioremediation of P-Nitrophenol by *Pseudomonas Putida*
1274 Strain. *J. Environ. Heal. Sci. Eng.* **2014**, *12* (1), 53.
<https://doi.org/10.1186/2052-336X-12-53>.
O’Connor, O. A.; Young, L. Y. Toxicity and Anaerobic
Biodegradability of Substituted Phenols under
Methanogenic Conditions. *Environ. Toxicol. Chem.* **1989**, *8*
(10), 853–862. <https://doi.org/10.1002/etc.5620081003>.
Gurevich, P.; Oren, A.; Sarig, S.; Henis, Y. Reduction of
Aromatic Nitro Compounds in Anaerobic Ecosystems.
Water Sci. Technol. **1993**, *27* (7–8), 89–96.
<https://doi.org/10.2166/wst.1993.0538>.